Terahertz-wave near-field imaging with subwavelength resolution using surface-wave-assisted bow-tie aperture

Kunihiko Ishihara[a] and Keishi Ohashi
Fundamental and Environmental Research Laboratories, NEC Corporation, 34 Miyukigaoka, Tsukuba, Ibaraki 305-8501, Japan

Tomofumi Ikari and Hiroaki Minamide
RIKEN Sendai, 519-1399 Aramaki Aoba, Aoba-ku, Sendai 980-0845, Japan

Hiroyuki Yokoyama
New Industry Creation Hatchery Center, Tohoku University, 10 Aramaki Aoba, Aoba-ku, Sendai 980-8579, Japan

Jun-ichi Shikata and Hiromasa Ito
Research Institute of Electrical Communication, Tohoku University, 2-1-1 Katahira, Aoba-ku, Sendai 980-8577, Japan

(Received 13 April 2006; accepted 30 September 2006; published online 17 November 2006)

We demonstrate the terahertz-wave near-field imaging with subwavelength resolution using a bow-tie shaped aperture surrounded by concentric periodic structures in a metal film. A subwavelength aperture with concentric periodic grooves, which are known as a bull's eye structure, shows extremely large enhanced transmission beyond the diffraction limit caused by the resonant excitation of surface waves. Additionally, a bow-tie aperture exhibits extraordinary field enhancement at the sharp tips of the metal, which enhances the transmission and the subwavelength spatial resolution. We introduced a bow-tie aperture to the bull's eye structure and achieved high spatial resolution ($\sim\lambda/17$) in the near-field region. The terahertz-wave near-field image of the subwavelength metal pattern (pattern width=20 μm) was obtained for the wavelength of 207 μm. © *2006 American Institute of Physics*. [DOI: 10.1063/1.2387984]

The demonstration of terahertz (THz) imaging has attracted much attention because of its many practical applications ranging from biomedical imaging to the inspection of semiconductor devices.[1] The spatial resolution of THz imaging, however, is limited by diffraction, and thus, only features with dimensions of hundreds of micrometers to millimeters can be distinguishable. To improve the spatial resolution, near-field imaging techniques, such as scanning near-field optical microscopy, have been applied to the THz region, and various methods based on this approach have been demonstrated.[2–6] A subwavelength aperture is one of the promising approaches to obtain subwavelength resolution. The main limitation of this method is the low transmission through the aperture, as most of the radiation is reflected at the aperture plane. According to standard aperture theory, transmission through a subwavelength aperture ($d \ll \lambda$) is proportional to d^6/λ^4, where d is the aperture diameter and λ is the wavelength of incident radiation.[7] This low transmission efficiency results in low sensitivity and it limits the spatial resolution.

Recently, a number of designs have been reported for subwavelength optics that obtain high spatial resolution and high power throughput simultaneously.[8–17] One takes advantage of the excitation of surface waves, often referred to as surface plasmon polaritons in the optical region, generated by using periodic structures.[8,9] A single subwavelength aperture surrounded by concentric periodic grooves, known as a bull's eye structure, shows extremely large enhanced transmission beyond the diffraction limit.[10,11] We have also reported on the bull's eye structure for the THz region and its application to THz-wave near-field imaging with subwavelength spatial resolution.[12,13] Another design uses various shapes of the aperture, such as C-,[14] I-,[15] or H-,[16] and bow-tie[16,17] shaped aperture. They have one feature in common, the small gap region formed by the ridge or ridges, which provide high transmission. In particular, a bow-tie aperture with sharp tips exhibits extraordinary field enhancement near the apex of the tips, resulting in extremely large transmission and subwavelength spot size.

In this letter, we propose to use the bow-tie aperture with the bull's eye structure. First, we analyze this structure by numerical simulation and then explain its fabrication and evaluation in detail. Finally, we describe the THz-wave near-field imaging of a subwavelength metal pattern with a spatial resolution below the diffraction limit.

Figure 1 is a schematic illustration of the bow-tie aperture with a bull's eye structure. The bull's eye structure consists of a thin metal film covering a substrate with concentric periodic grooves. The bow-tie aperture is arranged in the

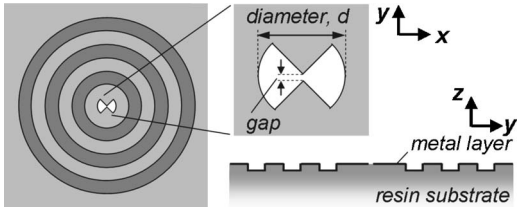

FIG. 1. Schematic illustration of bow-tie aperture with bull's eye structure. In the illustration, the number of concentric grooves (N) is 3, but $N=10$ was used in the fabricated one.

[a]Electronic mail: k-ishihara@da.jp.nec.com

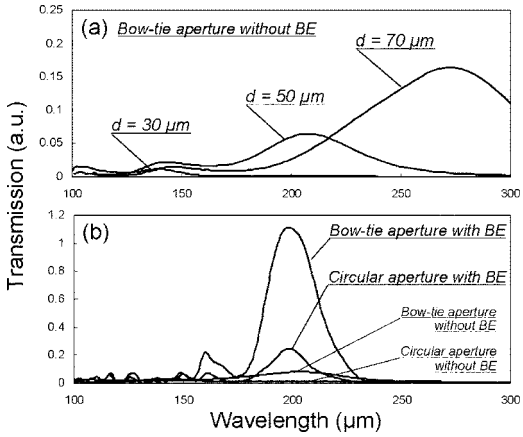

FIG. 2. Calculated transmission spectra for (a) bow-tie aperture without bull's eye (BE) with different values of aperture diameter d and for (b) bow-tie aperture and circular aperture with and without BE, with 50-μm-diameter aperture. BE consists of six periodic concentric grooves 66 μm wide and 13 μm deep with 132 μm periodicity on the resin substrate with a refractive index of 1.5 and is covered by a 2-μm-thick gold film. Bow-tie aperture gap is 6 μm. y-polarized wave is incident from substrate side.

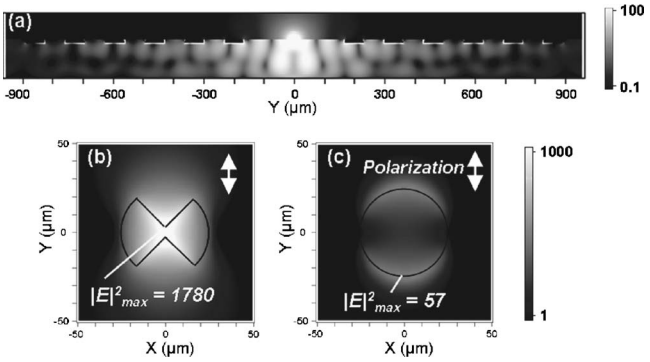

FIG. 3. (a) Calculated time-averaged $|E|^2$ distribution in logarithmic scale for bow-tie aperture with bull's eye in Fig. 2(b). y-polarized Gaussian beam at $\lambda = 198$ μm is incident to the z direction from bottom side (substrate side). (b) and (c) are distributions on the exit plane (x-y plane) at 2 μm distance from aperture for the bow-tie aperture and the circular aperture with bull's eye with 50-μm-diameter aperture, respectively.

metal film at the center of the concentric grooves. The substrate is transparent in the THz region and the incident THz-wave is illuminated from the substrate side.

First, we evaluated the effect of the bow-tie aperture in the bull's eye structure in an electromagnetic simulation using the three-dimensional finite-difference time-domain (FDTD) method. Figure 2 shows the calculated transmission spectra for the bow-tie aperture and the circular aperture with and without the bull's eye structure. The bow-tie aperture has been reported to have a peak in the transmission spectrum,[17] and its peak wavelength greatly depends on the aperture diameter, as shown in Fig. 2(a). The bull's eye structure also has a sharp resonant peak because of the resonant excitation of the surface waves caused by the periodic structure.[10–13] Therefore, we designed the bow-tie aperture with a bull's eye structure, as both peak wavelengths coincide. Figure 2(b) clearly shows that the bow-tie aperture with bull's eye has extremely large enhanced transmission peak. In particular, the bow-tie aperture with bull's eye exhibits higher transmission than the circular aperture with bull's eye (conventional bull's eye) though the bow-tie gap is 6 μm. This result is caused by the fact that the transmission of the single bow-tie aperture (without bull's eye) is several times as high as that of the single circular aperture.

The E-field distribution is useful in understanding the cause of this high transmission. Figure 3(a) shows the time-averaged $|E|^2$ distributions at a cross section through the center of a bow-tie aperture. The standing wave supported by the periodic grooves is built up on the substrate side and an extremely large E-field enhancement near the center is observed. This result can be explained by the fact that the incident wave couples to the surface mode, and the generated surface waves propagate to the center of the bull's eye. This phenomenon hardly depends on the aperture shapes. However, the $|E|^2$ distribution of the vicinity of the bow-tie aperture is greatly different from that of the circular aperture, as shown in Figs. 3(b) and 3(c). In the bow-tie aperture with bull's eye, a highly enhanced E field is observed at the apex of the tips, and the maximum intensity is 1780 times the incident intensity. This result indicates that the surface waves generated by the bull's eye structure are strongly scattered at the apex of the sharp tips and reradiated to the exit plane of the aperture. Consequently, the bow-tie aperture with bull's eye achieves the extremely large enhanced transmission through the narrow gap between the tips, and therefore, it is expected to realize a high spatial resolution for the application of the near-field imaging.

We fabricated a sample of the bow-tie aperture with a bull's eye structure. Figure 4(a) is a photograph of the sample. We first created ten concentric periodic grooves of 66 μm wide and 13 μm deep with 132 μm periodicity on a resin substrate (Tsurupica) using a diamond cutting tool. The resin substrate is transparent in the THz region and the refractive index is 1.5. Subsequently, a 0.4-μm-thick gold film was deposited using ion beam sputtering at a 45° angle. Finally, we fabricated the bow-tie aperture in the gold film at the center of the concentric grooves, which consists of 90° angle tips with a 5 μm gap in a 50-μm-diameter aperture, using the focused ion beam process. A THz-wave, which was generated by a THz-wave parametric oscillator (a widely tunable coherent THz-wave source),[18] was normally incident from the substrate side of the sample, and the transmission

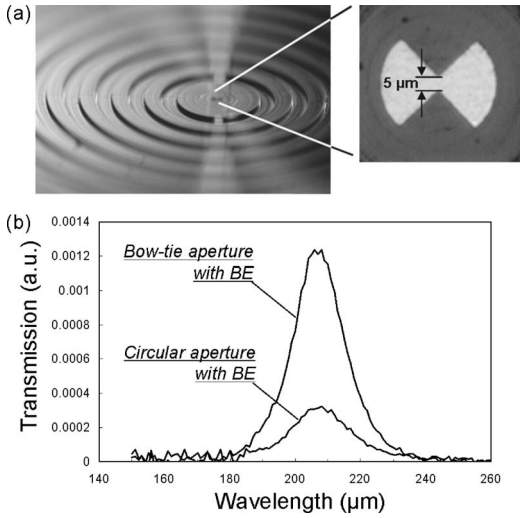

FIG. 4. (a) Photograph of bow-tie aperture with bull's eye, and (b) measured transmission spectra for bow-tie aperture with BE and circular aperture with BE (conventional bull's eye).

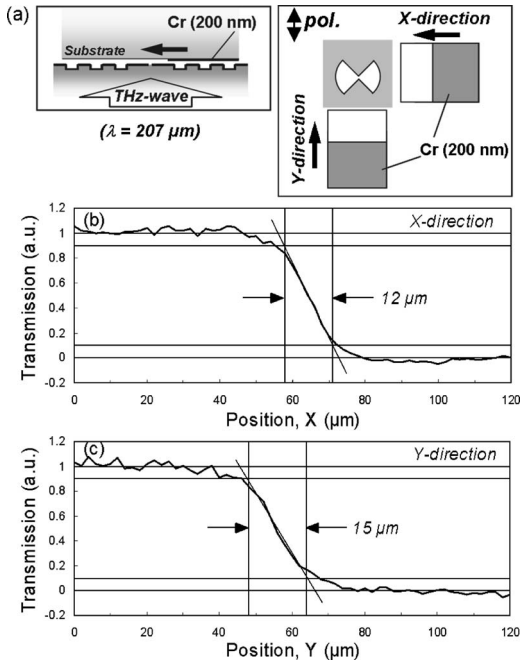

FIG. 5. (a) Schematic illustration of resolution test. (b) and (c) are the measured spatial resolution curves in the x direction and y direction, respectively.

power from the exit side of the aperture was detected by a 4 K Si bolometer.

Figure 4(b) shows the measured transmission spectra for samples of the bow-tie aperture with bull's eye and the circular aperture with bull's eye (the conventional bull's eye), with a 50-μm-diameter aperture. A larger enhanced transmission peak was observed in the bow-tie aperture with bull's eye compared with the conventional bull's eye.

To estimate the spatial resolution of the sample for the bow-tie aperture with bull's eye, we performed a resolution test by scanning a thin metal film edge across the bow-tie aperture. For this purpose, a 200-nm-thick Cr film was deposited on a resin substrate (Tsurupica). Figure 5(a) is a schematic illustration of the resolution test, which was performed in two directions for the bow-tie aperture. The separation between the metal film edge and the sample was about 10 μm. The wavelength of the incident THz-wave was fixed at 207 μm because the transmission peak was derived from the wavelength, as shown in Fig. 4. Figures 5(b) and 5(c) show the measured spatial resolution curves for the bow-tie aperture with bull's eye. In the x direction, we can quantify the spatial resolution as 12 μm (corresponding to $\lambda/17$) using the least squares approximation for a 10%–90% criterion of the transmission power and 15 μm for the y direction.

Finally, we describe the near-field imaging of a metal pattern using the bow-tie aperture with bull's eye. Figure 6 shows a two-dimensional scanning image of the metal pattern, which consists of a 200-nm-thick and 20-μm-wide Cr line deposited on a resin substrate, at a distance of about 10 μm. It clearly shows that the introduction of the bow-tie aperture to the bull's eye structure makes it possible to obtain a high-contrast image for the subwavelength structure because of its high spatial resolution as well as the extremely large enhanced transmission.

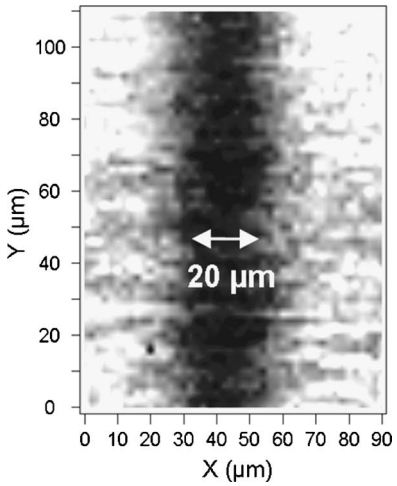

FIG. 6. THz-wave near-field image of 20-μm-wide Cr pattern using bow-tie aperture with bull's eye structure at wavelength of 207 μm. The image consists of 45×55 pixels with a 2×2 μm^2 pixel size.

In summary, we designed and introduced the bow-tie aperture to the surface-wave-assisted, enhanced transmission technique for THz-wave near-field imaging. A numerical simulation was performed, and the coincidence of both peak wavelengths of the bull's eye and the bow-tie aperture led to the extremely large enhanced transmission. The bow-tie aperture with bull's eye was fabricated and the spatial resolution of 12 μm (corresponding to $\lambda/17$) was achieved. Finally, we demonstrated two-dimensional THz-wave near-field imaging for the subwavelength metal pattern, resulting in a high-contrast image with high spatial resolution.

This work was performed as part of the Cooperative Research Project of the Research Institute of Electrical Communication, Tohoku University.

[1]B. B. Hu and M. C. Nuss, Opt. Lett. **20**, 1716 (1995).
[2]S. Hunsche, M. Koch, I. Brener, and M. C. Nuss, Opt. Commun. **150**, 22 (1998).
[3]Q. Chen, Z. Jiang, G. X. Xu, and X.-C. Zhang, Opt. Lett. **25**, 1122 (2000).
[4]O. Mitrofanov, M. Lee, J. W. P. Hsu, I. Brener, R. Harel, J. F. Federici, J. D. Wynn, L. N. Pfeiffer, and K. W. West, IEEE J. Sel. Top. Quantum Electron. **7**, 600 (2001).
[5]N. C. J. van der Valk and P. C. M. Planken, Appl. Phys. Lett. **81**, 1558 (2002).
[6]H.-T. Chen, R. Kersting, and G. C. Cho, Appl. Phys. Lett. **83**, 3009 (2003).
[7]H. A. Bethe, Phys. Rev. **66**, 163 (1944).
[8]T. W. Ebbesen, H. J. Lezec, H. F. Ghaemi, T. Thio, and P. A. Wolff, Nature (London) **391**, 667 (1998).
[9]W. L. Barnes, A. Dereux, and T. W. Ebbesen, Nature (London) **424**, 824 (2003).
[10]T. Thio, K. M. Pellerin, R. A. Linke, H. J. Lezec, and T. W. Ebbesen, Opt. Lett. **26**, 1972 (2001).
[11]H. J. Lezec, A. Degiron, E. Devaux, R. A. Linke, L. Martin-Moreno, F. J. Garcia-Vidal, and T. W. Ebbesen, Science **297**, 820 (2002).
[12]K. Ishihara, G. Hatakoshi, T. Ikari, H. Minamide, H. Ito, and K. Ohashi, Jpn. J. Appl. Phys., Part 2 **44**, L1005 (2005).
[13]K. Ishihara, T. Ikari, H. Minamide, J. Shikata, K. Ohashi, H. Yokoyama, and H. Ito, Jpn. J. Appl. Phys., Part 2 **44**, L929 (2005).
[14]X. Shi and Hesselink, Jpn. J. Appl. Phys., Part 1 **41**, 1632 (2002).
[15]K. Tanaka and M. Tanaka, J. Microsc. **210**, 294 (2002).
[16]E. X. Jin and X. Xu, Jpn. J. Appl. Phys., Part 1 **43**, 407 (2004).
[17]K. Sendur and W. Challener, J. Microsc. **210**, 279 (2002).
[18]K. Kawase, J. Shikata, and H. Ito, J. Phys. D **35**, R1 (2002).